



Cite this: *RSC Adv.*, 2016, 6, 17036

# Oxidative desulfurization of dibenzothiophene using a catalyst of molybdenum supported on modified medicinal stone

Lu Qiu,<sup>ab</sup> Yan Cheng,<sup>ab</sup> Chunping Yang,<sup>\*abc</sup> Guangming Zeng,<sup>ab</sup> Zhiyong Long,<sup>ab</sup> Sainan Wei,<sup>ab</sup> Kun Zhao<sup>ab</sup> and Le Luo<sup>ab</sup>

In this paper, the performance of catalytic oxidative desulfurization from model oil was studied using a catalyst of molybdenum supported on modified medicinal stone (Mo/MMS). The catalyst was successfully prepared by the sorption method and characterized by scanning electron microscopy (SEM), X-ray diffraction (XRD), Fourier transform infrared spectroscopy (FT-IR) and N<sub>2</sub> adsorption-desorption. The removal rate of dibenzothiophene (DBT) reached 97.5% within 60 min under conditions of catalyst dosage of 0.50 g, a reaction temperature of 100 °C, an oxidant/sulfur molar ratio (O/S) of 5.0 and the volume of model oil of 20 ml. The Box-Behnken design was used to evaluate the influence of the main operating parameters, including oxidation temperature (40–120 °C), oxidation time (40–80 min) and O/S (1.0–5.0) on DBT removal. The optimum values were found to be 103 °C, 62 min and 4.0, respectively. The removal rate of DBT reached a maximum at 98.1%. Statistical results also showed the degree of importance was: O/S > oxidation temperature > oxidation time. Sulfur removal dropped to 92.2% from 98.1% when the catalyst was reused 5 times. These results prove that the Mo/MMS catalyst could be cost-effective for removal of DBT from oil.

Received 3rd November 2015  
Accepted 2nd February 2016

DOI: 10.1039/c5ra23077b

[www.rsc.org/advances](http://www.rsc.org/advances)

## 1. Introduction

Sulfur compounds in oil can be converted to sulfur oxides (SO<sub>x</sub>), which lead to acid rain.<sup>1</sup> Sulfur can also deactivate catalysts fitted to an automotive exhaust purifier and shorten the service life of the engine. Because of an increase of environmental protection awareness and stringent legal requirements, ultra-deep desulfurization of fuels is attracting more and more attention.<sup>2</sup> In consequence, specific efforts are needed to produce more clean fuels,<sup>3</sup> and deep desulfurization techniques are needed worldwide.

Up to now, there are many alternative deep desulfurization techniques, such as oxidative desulfurization (ODS), hydro-desulfurization (HDS), biodesulfurization, adsorption, extraction and so on.<sup>2–4</sup> Conventional HDS is effective for thiols, sulfides and disulfides, but it can't effectively remove aromatic thiophenes, such as benzothiophene (BT), dibenzothiophene (DBT), 4,6-dimethyldibenzothiophene (4,6-DMDBT) and their alkylated derivatives,<sup>1,4–7</sup> because of their steric hindrance.<sup>5</sup> HDS

technologies require strict operating conditions including higher temperature, higher pressure, expensive hydrogen and a large amount of active catalysts to produce low sulfur oil.<sup>5,7–9</sup> In order to meet these requirements, costs for operating and maintenance are often too high. ODS has been considered as a promising new method for deep desulfurization of fossil oil.<sup>2</sup> In ODS, refractory organosulfur compounds are usually oxidized to the corresponding sulfones which are then removed by extraction, adsorption, distillation, or decomposition.<sup>2,9</sup> ODS is often carried out at the atmospheric pressure and moderate temperature as well as without using expensive hydrogen.<sup>2,10</sup>

In ODS, the final sulfur content still cannot meet the requirements of deep desulfurization without a catalyst.<sup>10</sup> The active components of catalysts are mainly composed of transition-metals, such as palladium, iridium, nickel, platinum, molybdenum, rhodium, titanium and tungsten.<sup>3,10–14</sup> Chica *et al.*<sup>14</sup> studied the activity and stability of Ti-MCM-41 catalyst for ODS in a continuous fixed-bed reactor, and it can achieved complete oxidation of DBT into DBT-sulfone. Molybdenum has been shown as an active catalyst in ODS in the form of molybdenum trioxide. For example, Han *et al.*<sup>10</sup> reported the oxidative desulfurization of DBT by phosphorous-modified MoO<sub>3</sub>/SiO<sub>2</sub> catalysts, and the sulfur removal rate reached 98.32%. Prasad *et al.*<sup>6</sup> found that Bi-modified MoO<sub>3</sub>/SiO<sub>2</sub>-Al<sub>2</sub>O<sub>3</sub> (1% SiO<sub>2</sub> : 99% Al<sub>2</sub>O<sub>3</sub>) showed the best catalytic performance compared to all the catalysts examined in the oxidation of 4,6-DMDBT.

<sup>a</sup>College of Environmental Science and Engineering, Hunan University, Changsha, Hunan 410082, P. R. China. E-mail: yangc@hnu.edu.cn

<sup>b</sup>Key Laboratory of Environmental Biology and Pollution Control (Hunan University), Ministry of Education, Changsha, Hunan 410082, P. R. China

<sup>c</sup>Zhejiang Provincial Key Laboratory of Solid Waste Treatment and Recycling, College of Environmental Science and Engineering, Zhejiang Gongshang University, Hangzhou, Zhejiang 310018, P. R. China

Supports of catalyst such as silica, activated carbon, alumina, resins and molecular sieves<sup>2,3,9-15</sup> play an important role in ODS. These supports can improve the activity of catalysts and promote the separation of catalysts from reaction systems. However, some supports are either expensive or complex for preparation. In recent years, medicinal stone has gained much attention due to its some special properties, such as the sponge structure, special porous and relatively large specific surface area.<sup>16</sup> The porous medicinal stone with 10 nm aperture has huge specific surface area and can be used as an excellent absorbent.<sup>17</sup> Medicinal stone is a cheap and readily available mineral substance. The main chemical components are SiO<sub>2</sub>, Al<sub>2</sub>O<sub>3</sub>, Fe<sub>2</sub>O<sub>3</sub>, CaO, MgO, K<sub>2</sub>O, Na<sub>2</sub>O, *etc.*<sup>18</sup> Then it is easy for us to infer that the medicinal stone could be used as the support of catalyst in ODS.

The aim of this work is to prepare, characterize and evaluate a cost-effective catalyst for ODS. Molybdenum was chosen as a catalyst, and modified medicinal stone (MMS) was used as the support. The influences of various factors including reaction temperature, reaction time, oxidant/sulfur molar ratio and the amount of catalyst were evaluated. The reuse of the catalyst was also examined. The Box–Behnken design was selected to determine the optimum conditions for ODS and to illustrate the relations between sulfur removal and three independent variables including oxidation temperature, oxidation time, and oxidant/sulfur molar ratio. The results are supposed to show the feasibility of the catalytic oxidative desulfurization system for DBT removal.

## 2. Experimental

### 2.1. Materials

DBT (analytical-grade reagent, AR) was obtained from Acros Organics Co. Ltd; *n*-octane (AR) was used as solvent of model compounds and it was purchased from Tianjin Kemiou Chemical Reagent Co. Ltd; cyclohexanone peroxide (CYHPO) as oxidant agents, *N,N*-dimethylformamide (DMF) as extracting agent and ammonium molybdate (AR) were purchased from Sinopharm Chemical Reagent Co. Ltd. (China); medicinal stone was produced from Tongliao Inner Mongolia (China). All compounds were used without further treatment.

### 2.2. Catalyst preparation and characterization

The catalyst was prepared by a sorption method.<sup>16</sup> The preparation procedure was as follows: firstly, the medicinal stone (MS) was calcined at 500 °C in air for 2 h. Subsequently, the medicinal stone were macerated in 1.0 mol L<sup>-1</sup> of hydrochloric acid for 24 h. Then, 4.0 g of ammonium molybdate was dissolved in the 20 ml of deionized water, and the solution was used for the impregnation of 5.0 g of the modified medicinal stone (MMS). Finally, the mixture was stirred for 3 h, and then aged at room temperature for 12 h without stirring. The solid products were obtained by filtration, washed with deionized water and dried at 105 °C. Calcination was carried out in static air at 500 °C for 2 h. Each time, the loading amount of metals on

support was 4.7 wt% approximately and the catalyst was named as Mo/MMS catalyst in this study.

The catalyst was characterized by powder X-ray diffraction (XRD) using a Rigaku Dmax 2500 diffractometer equipped with a monochromator and a Cu target tube to investigate the crystal structure of the samples. A scanning electron microscope (SEM) study of the samples was performed using a Hitachi S-4800 electron microscope in order to observe the surface morphology of the Mo/MMS catalyst and MMS. The Fourier transform infrared spectrometer (FT-IR) experiments were operated on FTIR spectrophotometer (VARIAN 3100 FTIR) with the frequency range of 400–4000 cm<sup>-1</sup>. The samples were diluted with KBr and pressed into flakes. Spectra were obtained at the resolution of 4 cm<sup>-1</sup> and room temperature. Textural properties of the samples were obtained by N<sub>2</sub> adsorption–desorption isotherms (Micromeritics Tristar II 3020). Specific surface areas were calculated by the BET method, the total pore volume was obtained by nitrogen adsorption at a relative pressure of 0.98 and pore size distribution was analyzed from the desorption isotherms and calculated by the BJH method. The molybdenum content of the catalyst was measured by inductively coupled plasma-atomic emission spectrometry (ICP-AES) (Perkin Elmer Optima 3300DV).

### 2.3. Catalytic performance test

This experimental procedure consisted of oxidation and extraction. Specific operation process was as follows: firstly, model oil was obtained *via* dissolving DBT in the *n*-octane.<sup>19</sup> The S-content was 500 ppm. 20.0 ml of model oil was added into the Erlenmeyer flask (250 ml), and then 0.50 g of Mo/MMS catalyst and 0.2309 g of CYHPO (O/S of 3.0) were also added into the reactor respectively. Then, the reactor was fixed in an oil bath at different constant temperature and equipped with a magnetic stir bar.<sup>11</sup> The oxidation reaction was carried out at atmospheric pressure. After 40 min of reaction, the mixture was left at room temperature without stirring for 0.5 h in order to attain phase separation. The following step was to filter the oxidized oil. Subsequently, the oxidized oil was extracted two times each with 10 ml DMF<sup>20</sup> in order to obtain low sulfur oil. Following the end of a reaction, the used catalysts were separated from the reaction system, washed with methanol. Then the catalysts were treated in vacuum oven at 105 °C for 12 h before being used again.

### 2.4. Analysis

The sulfur content of samples was analyzed by gas chromatography (GC) (Agilent 6890 N; HP-5, 30 m × 0.32 mm × 0.25 μm; FID: Agilent). The sulfur removal in the model oil was utilized to show the performance of the catalyst and the results in this study were calculated based on the following:

$$\eta = [(C_0 - C)/C_0] \times 100\% \quad (1)$$

where  $\eta$  represents the sulfur removal rate,  $C_0$  and  $C$  denote as the initial and final concentration of sulfur in the model oil, respectively.

Table 1 Experimental values and level of independent variables

Independent variables	Code	Range and levels		
		-1	0	1
Oxidation temperature (°C)	$X_1$	40	80	120
Oxidation time (min)	$X_2$	40	60	80
Oxidant/sulfur ratio	$X_3$	1.0	3.0	5.0

Table 2 Experimental designs and actual and predicted response values for the Box–Behnken design

Run	Coded values			Actual values			Sulfur removal (%)		
	$X_1$	$X_2$	$X_3$	$X_1$	$X_2$	$X_3$	Actual	Predicted	Residual
1	-1	0	-1	40	60	1.0	82.10	81.40	0.70
2	1	-1	0	120	40	3.0	94.00	93.53	0.47
3	0	0	0	80	60	3.0	96.89	96.94	-0.052
4	0	1	1	80	80	5.0	94.72	94.37	0.35
5	0	1	-1	80	80	1.0	84.23	84.46	-0.35
6	0	0	0	80	60	3.0	96.73	96.94	-0.21
7	-1	0	1	40	60	5.0	87.37	87.25	0.12
8	0	-1	-1	80	40	1.0	83.65	84.00	-0.35
9	-1	-1	0	40	40	3.0	86.40	86.75	-0.35
10	1	0	1	120	60	5.0	96.85	97.55	-0.70
11	0	-1	1	80	40	5.0	93.20	92.97	0.23
12	1	0	-1	120	60	1.0	84.40	84.52	-0.12
13	0	0	0	80	60	3.0	97.00	96.94	0.058
14	1	1	0	120	80	3.0	94.73	94.38	0.35
15	0	0	0	80	60	3.0	96.99	96.94	0.048
16	0	0	0	80	60	3.0	97.10	96.94	0.16
17	-1	1	0	40	80	3.0	87.30	87.76	-0.46

The recovery of model oil was calculated using the following relationships:

$$\varepsilon = [(m_0 - m)/m_0] \times 100\% \quad (2)$$

where  $\varepsilon$  represents the recovery rate of model oil,  $m_0$  and  $m$  denote as the initial and final weight of model oil, respectively.

## 2.5. Design of experiment with Box–Behnken method

Response surface methodology (RSM) has been widely used for the optimization and verification of scientific researches and industrial studies.<sup>20</sup> Box–Behnken design is one of the experimental design methods in RSM. With this design, more information can be obtained from a minimum number of

Table 3 Texture properties of the samples

Samples	BET area ( $\text{m}^2 \text{g}^{-1}$ )	Average pore size (nm)	Pore volume ( $\text{cm}^3 \text{g}^{-1}$ )
MS	54.3	22.4	0.30
MMS	75.6	23.1	0.43
Mo/MMS catalyst	68.3	21.5	0.34

experiences, and the data indicate the interactions among the factors.<sup>21,22</sup>

In this study, response surface methodology was used for statistical analysis of the experimental data using Design Expert software version 8.0.5. The influence of main factors included oxidation temperature  $X_1$  (40–120 °C), oxidation time  $X_2$  (40–80 min) and O/S  $X_3$  (1–5). As shown in Table 1, each variable was coded at three levels: 1, 0, and -1, which represented the high level, center point and low level, respectively. A total of 17 experiments and the results were summarized in Table 2. A second-order model in the form of quadratic polynomial equation was used for the optimization process.<sup>23</sup>

$$Y = \beta_0 + \sum \beta_i x_i + \sum \beta_{ii} x_i^2 + \sum \beta_{ij} x_i x_j$$

where  $Y$  is the response variable to be modeled;  $\beta_0$ ,  $\beta_i$ ,  $\beta_{ii}$  and  $\beta_{ij}$  are constant term, linear coefficient, quadratic coefficient and second order interaction coefficient, respectively;  $x_i$  and  $x_j$  are independent variables which determine  $Y$ .  $F$ -Test and  $t$ -test were used for judging the statistical significance of the model and the coefficients respectively. In addition, the interaction of the independent variables was researched by constructing the response surface and contour plot.<sup>22,23</sup>

## 3. Results and discussion

### 3.1. Characterization of Mo/MMS catalyst

In order to investigate the properties of the catalysts, various characteristics have been taken. SEM provided useful information for understanding the morphology difference<sup>24</sup> between Mo/MMS catalyst and the support (MMS) (Fig. 1). It can be seen from Fig. 1(a and b) that the medicinal stone had porous sponge and typical laminated structure. The results agreed with Yan *et al.* reported.<sup>16</sup> The shape of MMS was formed might be due to weathering altered the natural structure of medicinal stone. Fig. 1(c and d) showed the surface of MMS had many small particles, causing the surface morphology was much rough.

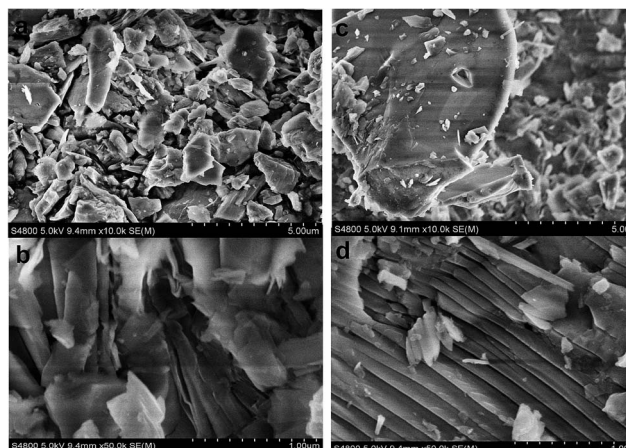


Fig. 1 SEM images of: (a and b) modified medicinal stone, (c and d) Mo/MMS catalyst.

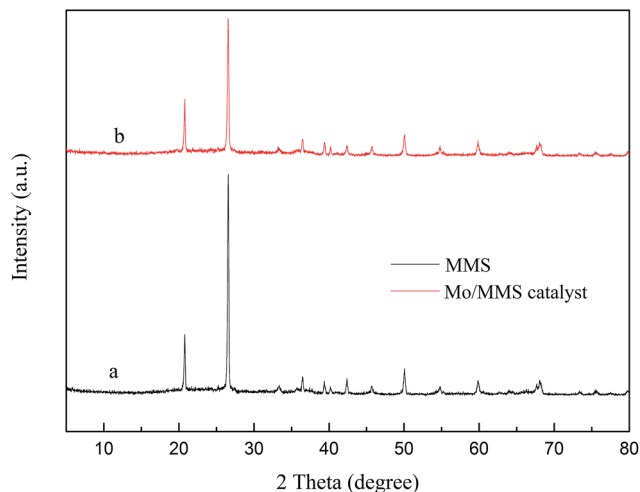


Fig. 2 X-ray diffractograms of: (a) modified medicinal stone and (b) Mo/MMS catalyst.

This finding indicated that immobilization of molybdenum on MMS influenced its morphology.

Powder XRD patterns of MMS and Mo/MMS catalyst were shown in Fig. 2. As seen in Fig. 2, all samples showed some sharp peaks at approximately  $20.69^\circ$  and  $26.65^\circ$ , which were attributed to the crystalline silica. The XRD patterns of these samples were exactly similar, and no sharp peaks of  $\text{MoO}_3$  were found in the patterns. It indicated that MMS structures didn't change and metal species were well dispersed on the surface of MMS. The results obtained on Mo/MMS catalyst agreed with the literature reported.<sup>16</sup> However, Mo/MMS catalyst presented a significant decrease in the intensity of the diffraction peaks compared with MMS it could be due to the absorption coefficient of impregnated metal species.<sup>25</sup>

FT-IR spectra of the Mo/MMS catalyst and MMS were depicted in Fig. 3. As shown in Fig. 3, the samples supported  $\text{MoO}_3$  maintained the characteristic peaks of MMS. Typical

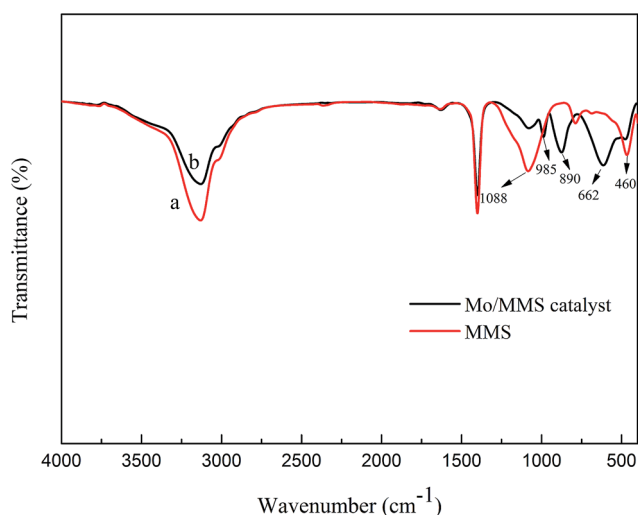


Fig. 3 FTIR of: (a) modified medicinal stone and (b) Mo/MMS catalyst.

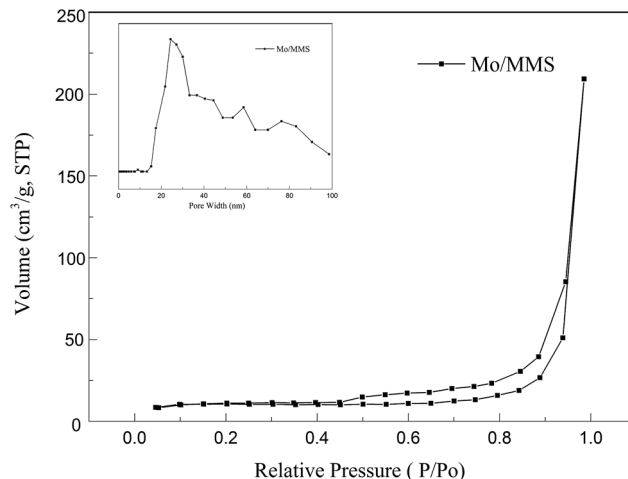


Fig. 4 Nitrogen adsorption-desorption isotherms of Mo/MMS catalyst.

peaks of Si-O-Si could be observed at  $1088\text{ cm}^{-1}$  and  $460\text{ cm}^{-1}$ .<sup>19,26</sup> This vibration corresponded to the Si-O-Si bonds in the all of the samples. Meanwhile, it can be seen that the FTIR spectrum of Mo/MMS catalyst showed three distinct absorption bands:  $985\text{ cm}^{-1}$  (Mo-O-Mo symmetric stretch),  $890\text{ cm}^{-1}$  (Mo-O-Mo asymmetric stretch) and  $662\text{ cm}^{-1}$  (terminal Mo=O stretch), which could be assigned to molybdenum trioxide.<sup>12,15</sup> It indicated that the metal might has been load in the support. This result was consistent with the observation from SEM (Fig. 1).

Some structure parameters of all samples (MS, MMS and Mo/MMS catalyst) were summarized in Table 3. The surface area is  $54.3\text{ m}^2\text{ g}^{-1}$  for MS. The surface area and pore volume of MMS was larger than that of MS, indicating that MS was successfully modified. Compared with MMS, the surface area of Mo/MMS catalyst decreased slightly; average pore size and total pore

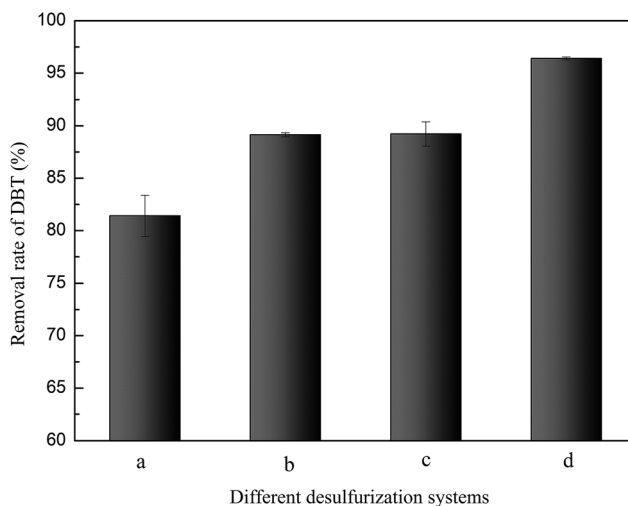


Fig. 5 Different desulfurization systems: (a) DBT has not been oxidized; (b) DBT was oxidized by CYHPO without catalyst; (c) DBT was oxidized by CYHPO with MMS; (d) DBT was oxidized by CYHPO with Mo/MMS catalyst.

volume also decreased. These decrements in the textural properties may be related with molybdenum loading in MMS.<sup>15</sup> The adsorption–desorption isotherm of Mo/MMS catalyst was presented in Fig. 4. The features of Mo/MMS catalyst isotherm can be attributed to IV adsorption isotherm according to IUPAC classification, characterizing the presence of mesopores.<sup>27</sup> The isotherm showed a H3 hysteresis loop, typical for materials with slit shape pores of non-uniform size or shape.<sup>5</sup> The inset of Fig. 4 illustrated the pore size distribution. A pore size distribution with maximum at 20 nm can be observed. The molecular diameter of DBT is much smaller than the pore diameter of the catalyst. Therefore, the pore of the catalyst is enough to allow DBT molecules to diffuse into the pores where most of the active sites for ODS are located.

### 3.2. DBT removal at different desulfurization systems

In order to demonstrate the high catalytic activity of Mo/MMS catalyst, four groups of desulfurization systems in this paper were investigated: (a) DBT has not been oxidized; (b) DBT was oxidized by CYHPO without catalyst; (c) DBT was oxidized by CYHPO with MMS; (d) DBT was oxidized by CYHPO with Mo/MMS catalyst. All experiments were carried out under the same operating conditions: catalyst dosage of 0.50 g, temperature of 100 °C, O/S of 3.0, time of 40 min and the volume of model oil of 20 ml. Subsequently, samples were extracted by DMF. The results were shown in Fig. 5. It can be seen that the removal rate of DBT was only 82.8% in the absence of oxidant CYHPO, and the result was similar to the report of Mokhtar *et al.*<sup>20</sup> When DBT was oxidized by CYHPO without catalyst, 89.3% DBT removal was achieved. Therefore, CYHPO played an important part in the oxidation reaction. When the Mo/MMS catalyst was added, the removal rate of DBT was up to 96.5%, indicating that Mo/MMS catalyst displayed a very high catalytic oxidative desulfurization activity for DBT. Similar results were reported by Abdullah *et al.*<sup>2</sup> and Han *et al.*,<sup>10</sup> indicating that MoO<sub>3</sub> showed excellent efficiency for DBT removal. Zhou *et al.*<sup>28</sup> studied the catalytic oxidation of DBT using CYHPO with MoO<sub>3</sub>/D113 catalyst and the

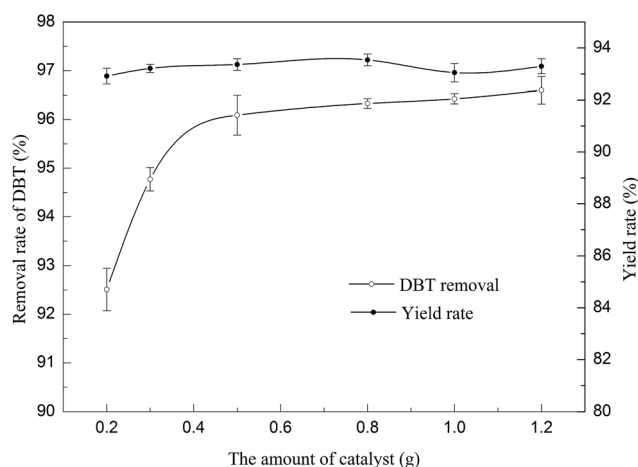


Fig. 6 Effect of the amount of catalyst on DBT removal and the yield rate of model oil. Conditions: temperature of 100 °C, O/S of 3.0, time of 40 min and the volume of model oil of 20 ml.

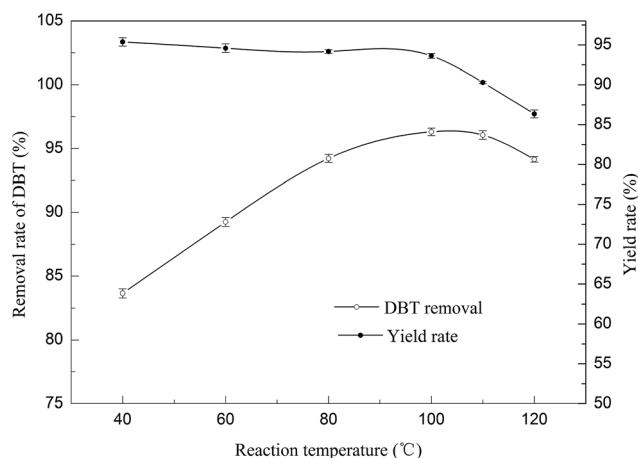


Fig. 7 Effect of reaction temperature on DBT removal and the yield rate of model oil. Conditions: catalyst dosage of 0.50 g, O/S of 3.0, time of 40 min and the volume of model oil of 20 ml.

desulfurization rate reached 100%. According to Zhou *et al.*<sup>28</sup> the role of MoO<sub>3</sub> in the catalyst was to increase the electrophilicity of peroxy oxygen, so DBT could be rapidly oxidized to sulfones at the presence of Mo/MMS catalyst. In the next experiment, optimum operating conditions were studied.

### 3.3. Effects of reaction conditions on DBT removal

**3.3.1. Effect of amount of catalyst.** The amount of the catalyst is an important factor for oxidative desulfurization. As can be seen in Fig. 6, the sulfur removal enhanced gradually with the increase of the catalyst dosage, and then tended to be balanced. As the amount of catalyst increased from 0.20 g to 0.50 g, the removal rate of DBT rose from 92.7% to 96.1%. Because more catalyst dosage could provide more active center and more opportunity for DBT contacted with catalyst, which would make DBT more easily to be oxidized and removed. However, further increasing of catalyst dosage to 1.0 g, the sulfur removal did not change appreciably. It might be due to the number of active center was excessed and most DBT could be fully oxidized. Similar tendency was also observed in removal of DBT and BT by mesoporous H<sub>3</sub>PMo<sub>12</sub>O<sub>40</sub>/SiO<sub>2</sub>.<sup>29</sup> In addition, the yield rate of model oil changed little at the various catalyst dosages evaluated (Fig. 5). Therefore, 0.50 g was chosen as the suitable amount of catalyst in further experiments.

**3.3.2. Effect of reaction temperature.** To evaluate the role of the reaction temperature, the oxidation was carried out at different temperatures, ranging from 40 °C to 120 °C and the results were shown in Fig. 7. It is obvious that the oxidative ability toward sulfide was strengthened with the increasing of reaction temperature. The oxidative removal of DBT increased dramatically from 83.8% to 96.4% with the increase of temperature from 40 °C to 100 °C in 40 min. The reason for this phenomenon might be that an increase of temperature led to the movement of molecular speeding up, increasing the reaction probability between sulfur compounds and oxidant.<sup>2</sup> Nevertheless, when the reaction temperature was over 105 °C, the oxidative removal of DBT decreased sharply. It was ascribed

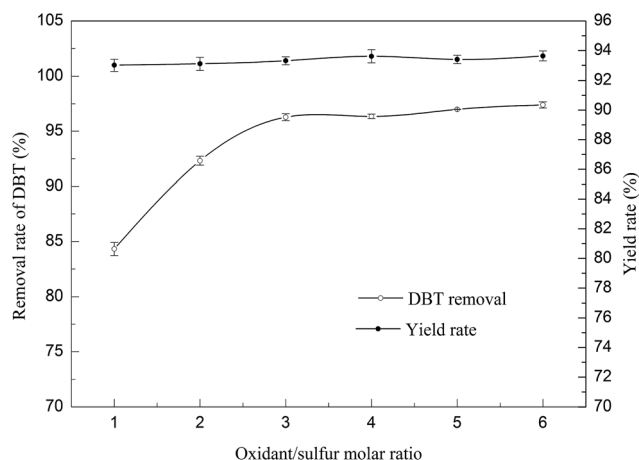


Fig. 8 Effect of oxidant/sulfur molar ratio on DBT removal and the yield rate of model oil. Conditions: catalyst dosage of 0.50 g, temperature of 100 °C, time of 40 min and the volume of model oil of 20 ml.

to that more CYHPO was decomposed under higher reaction temperature.<sup>28</sup> Zang *et al.*<sup>30</sup> also found that the CYHPO was decomposed at 100–120 °C.

Besides, the yield rate of model oil was also affected by temperature (Fig. 7). As the temperature increased from 40 °C to 120 °C, the yield rate of model oil declined sharply from 95.1% to 86.4%. Obviously, model oil lost due to volatilization and gasification at higher temperatures. Hence, the temperature of 100 °C presented the best desulfurization result.

**3.3.3. Effect of oxidant/sulfur molar ratio.** To investigate the influence of oxidation dosage on oxidative desulfurization by Mo/MMS catalyst, a series of experiments with varying O/S (1–5) were carried out under the same reaction conditions. As seen in Fig. 8, when O/S was 2.0, the removal rate of DBT was 92.2%. While O/S rose to 4.0 and 5.0, DBT removal reached 96.2% and 97.0% at 40 min, respectively. However, further increasing O/S, the removal rate of sulfur increased slightly. According to the stoichiometry of the reaction, in theory, 1 mol DBT would consume 2 mol CYHPO and produce 1 mol sulfone. As previously reported,<sup>1,4</sup> O/S was usually over 2.0 in the actual reaction process because there were two competitive reactions between the oxidation of DBT by CYHPO and the self-decomposition of CYHPO.<sup>4</sup> Besides, the yield rate of model oil was consistent nearly (Fig. 8). In consideration of the cost of CYHPO and the effect of desulfurization in reaction system, O/S of 5.0 was a suitable choice for the consequent experiments, somewhat lower than that used in previously reported studies.<sup>31,32</sup>

**3.3.4. Effect of reaction time.** The effect of different reaction time (40–100 min) on desulfurization of the model oil were shown in Fig. 9. The same reaction conditions were: catalyst dosage of 0.50 g, temperature of 100 °C, O/S of 5.0 and the volume of model oil of 20 ml. It can be seen from Fig. 9 that the yield rate of model oil declined slightly in the first 60 min. Subsequently, the yield rate decreased from 93.2% to 89.3% with the increase of time. A reason of these results might be the occurrence of volatilization of the model oil. However, the effect

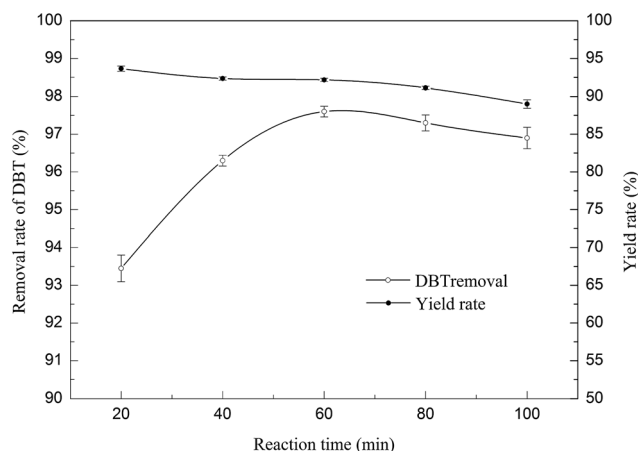


Fig. 9 Effect of reaction time on DBT removal and the yield rate of model oil. Conditions: catalyst dosage of 0.50 g, temperature of 100 °C, O/S of 5.0 and the volume of model oil of 20 ml.

of volatilization on the conversion of DBT was not so significant at a shorter reaction time of 60 min. At first, the removal rate of DBT was very low because the reaction was not complete. It is obvious that the desulfurization rates increased along with the reaction time. The removal rate of DBT reached 97.5% in 60 min and then slightly decreases beyond this value. Therefore, further increasing the reaction time is not significant in increasing the removal rate of sulfur. Gutiérrez *et al.*<sup>12</sup> reported that 86.0% removal of sulfur in diesel fuel was achieved after 60 min and 97.8% sulfur removal was achieved at 75 min of reaction when catalyst Mo/Al<sub>2</sub>O<sub>3</sub> was used. Xie *et al.*<sup>1</sup> reported the majority of DBT conversion completed within 30 min, and DBT was almost completely converted (>99%) after 180 min when used MCM-41-NH<sub>2</sub>/Q<sub>4</sub>-H<sub>2</sub>Se<sub>3</sub><sup>IV</sup>W<sub>6</sub> as the catalyst. Based on the above discussion, 60 min was a proper time for the requirement of deep desulfurization.

### 3.4. Statistical analysis and optimization by Box–Behnken design

All results obtained from the BBD experimental design were summarized in Table 2. From these data, the quadratic model was used to explain the mathematical relationship between the response and three selected parameters, which was expressed by:

$$Y = 96.94 + 3.35X_1 + 0.47X_2 + 4.72X_3 - 0.043X_1X_2 + 1.79X_1X_3 + 0.23X_2X_3 - 3.08X_1^2 - 2.53X_2^2 - 5.46X_3^2$$

The results of analysis of variance (ANOVA) were presented in Table 4. The significance of each parameter was evaluated by the calculated Fischer values (*F*-test) and probability values (*p*-value). The corresponding parameter is more significant if its *p*-value is smaller than 0.05 at 95% confidence level.<sup>22,33</sup> Obviously, as shown in Table 4, the model *F*-value of 192.08 and values of “Prob > *F*” less than 0.0001 indicated the model was significant. There was only a 0.26% chance that a “Model *F*-Value” this large could

**Table 4** ANOVA results of the quadratic model for the oxidative desulfurization using Mo/MMS catalyst<sup>a</sup>

Source	SS	DF	MS	F	p
Model	518.37	9	57.60	192.08	<0.0001
Oxidation temperature, $X_1$	89.85	1	89.85	299.63	<0.0001
Oxidation time, $X_2$	1.74	1	1.74	5.80	0.0469
O/S, $X_3$	178.23	1	178.23	594.37	<0.0001
$X_1X_2$	7.225 × 10 <sup>-3</sup>	1	7.225 × 10 <sup>-3</sup>	0.024	0.8810
$X_1X_3$	12.89	1	12.89	42.98	0.0003
$X_2X_3$	0.22	1	0.22	0.74	0.4191
$X_1^2$	60.87	1	60.87	203.00	<0.0001
$X_2^2$	27.00	1	27.00	90.04	<0.0001
$X_3^2$	125.51	1	125.51	418.57	<0.0001
Residual	2.10	7	0.30		
Lack of fit	2.02	3	0.67	34.42	0.0026
Pure error	0.078	4	0.020		
Total	520.47	16			
R-Squared	Adj R-squared		Pred R-squared		
0.9960	0.9908		0.9376		

<sup>a</sup> DF: degree of freedom of different source; SS: sum of square, MS: mean of square; F: degree of freedom; P: probability.

occur due to noise. The “Lack of Fit  $F$ -value” of 34.42 implied the lack of fit was significant. In this study, the independent variables of the quadratic model oxidation temperature  $X_1$ , oxidation time  $X_2$  and O/S  $X_3$ , the interaction between temperature and O/S ( $X_2X_3$ ) and the interaction between time and O/S ( $X_1X_3$ ) were quite significant because the  $p$ -value was less than 0.05. Judging by the  $F$ -values of the items in the regression model, the oxidant/sulfur ratio ( $X_3$ ) had the highest  $F$ -value (594.37) with lowest  $p$ -value (<0.0001) among other parameters, so the order in which the independent parameters influenced the oxidative desulfurization efficiency was: O/S  $X_3$  > oxidation temperature  $X_1$  > oxidation time  $X_2$ .

The accuracy of the model was determined by the residual analysis. The comparison between the removal rate of sulfur, obtained from the empirical model, and observed experimental data was presented in Fig. 10(a). According to previous studies,<sup>20</sup> both of the coefficients of determination,  $R^2$  and adjusted  $R^2$  should be at least 0.80 for a better fit of a model. In this case, the coefficient of determination ( $R^2$ ) of the regression model was 0.9960 (Fig. 10(a)), meaning that more than 99.60% of the data deviation could be explained by the empirical model, which showed that the regression model was statistically significant. Besides, the  $R^2$ -Adj value was 99.08%, indicating that the experimental results were in good agreement with the predicted

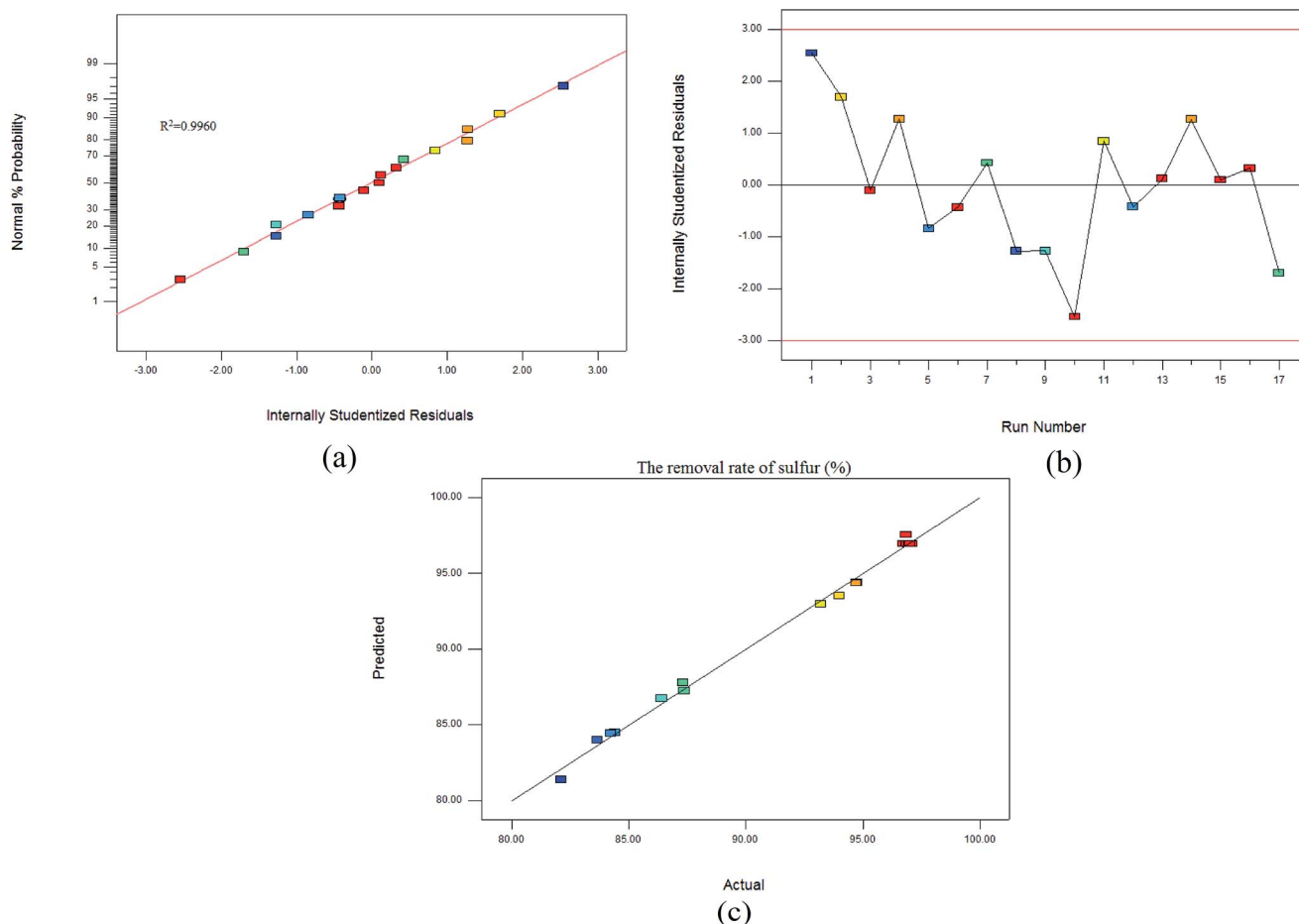


**Fig. 10** Residual plots of the predicted model for the removal rate of DBT: (a) predicted values versus the actual response, (b) residual versus run numbers and (c) normal probability plot of residuals.

values. Fig. 10(b) illustrated the normal probability plot of the residual. Obviously, the acquired data points appeared on a linear relationship consistently, which indicated the random error was independently and normally distributed. The residual plot *versus* run number was presented in Fig. 10(c). The random residuals were distributed around the line, which showed that

model was appropriate. In addition, the adequacy of the model could be evaluated by the residuals calculated by determining the difference between the experimental and the predicted the removal rate of sulfur.

In this study, response surfaces can be visualized as contours and 3D plots which obtained from the predicted models. The

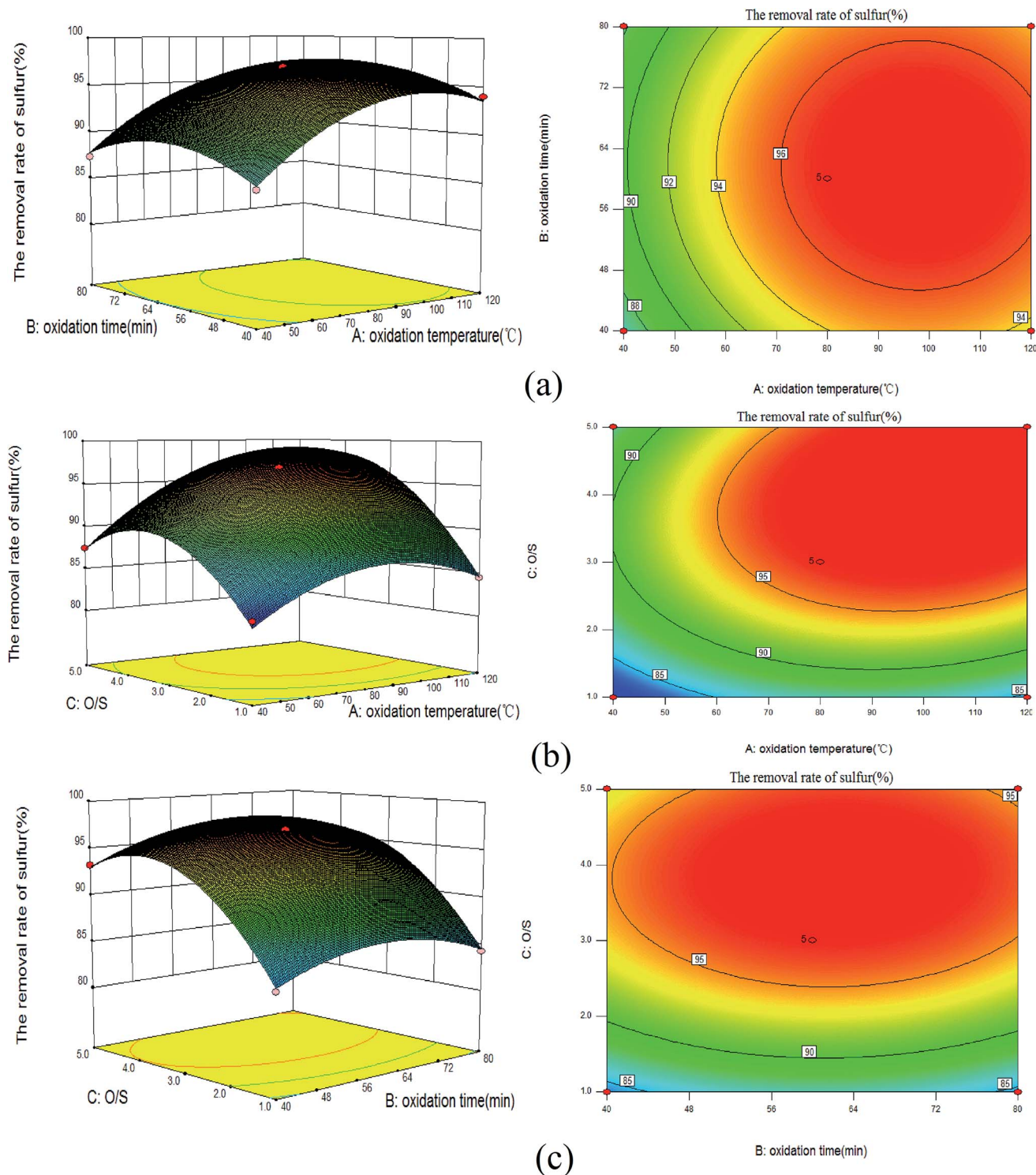


Fig. 11 Contours and 3D surface plots of the removal rate of DBT for: (a) oxidation temperature and oxidation time, (b) oxidation temperature and O/S and (c) oxidation time and O/S.

resulting of both contours and 3D surface response plots demonstrated the variation of the response with two independent variables while holding the other variable fixed, as a function of (a) oxidation temperature and oxidation time ( $O/S = 3.0$ ), (b) oxidation temperature and  $O/S$  ( $t = 60$  min) and (c) oxidation time and  $O/S$  ( $T = 80$  °C), respectively. The results were presented in Fig. 10. The elliptical form of each contour plot can help to understand the effect of various interactions on sulfur removal and also to determine optimum level of each variable.

As can be seen in Fig. 11(a), at the lower oxidation time, sulfur removal decreased gradually at the lower or higher of the oxidation temperature. Also, when a high level of temperature was applied (120 °C), the removal rate of sulfur was found to climb up and then decline by increasing time of reaction. From these results, the maximum sulfur removal (>96.03%) was observed in the region where the oxidation time was limited to  $45 < t < 75$  min at a moderate level of temperature ( $88$  °C <  $T < 98$  °C). An appropriate increase in temperature caused the molecular movement to speed up and increased the reaction probability between oxidant and sulfur compounds. Fig. 11(b) represented response surface plot of two variables oxidation temperature and  $O/S$  while oxidation time was kept constant at 60 min. The highest sulfur removal (>96.03%) occurred when  $O/S$  and oxidation temperature were kept at about 2.5–5.0 and 70–96 °C, respectively. It was obvious that the variation of  $O/S$  is more important than oxidation temperature. The reason may be that lessen of oxidant concentration would cause an incomplete conversion of the sulfur compounds to sulfone or sulfoxide. Fig. 11(c) illustrated the effect of oxidation time and  $O/S$  on sulfur removal at the oxidation temperature of 80 °C. It was obvious that at a low level of oxidant ratio, sulfur removal was consistent nearly with increasing time of reaction and similar results were obtained by Mokhtar *et al.*<sup>22</sup> It has been seen that the variation of oxidant ratio has a significant impact on the removal rate of sulfur, while the variation of oxidation time was less important. From these results, it could be summarized that the degree of importance of these variables on sulfur removal was: oxidant/sulfur molar ratio > oxidation temperature > oxidation time, which was the same as the previous result.

The optimized conditions for three main parameters: oxidant/sulfur molar ratio, oxidation temperature and time were obtained by response optimizer. The values of the independent variables for the maximum removal rate of sulfur were presented in Table 5. The predicted response (sulfur removal) was found to be 99.0%, under the optimum conditions: oxidation temperature of 103 °C, oxidation time of 62 min and  $O/S$  of 4.0, respectively. The predicted conditions were validated by conducting an experiment thrice for the reproducibility of the

Table 5 Values of the process parameter for maximum sulfur removal

Parameter	Values
Sulfur removal (%)	99.0
$X_1$ (oxidation temperature, °C)	103
$X_2$ (oxidation time, min)	62
$X_3$ (oxidant/sulfur ratio)	4.0

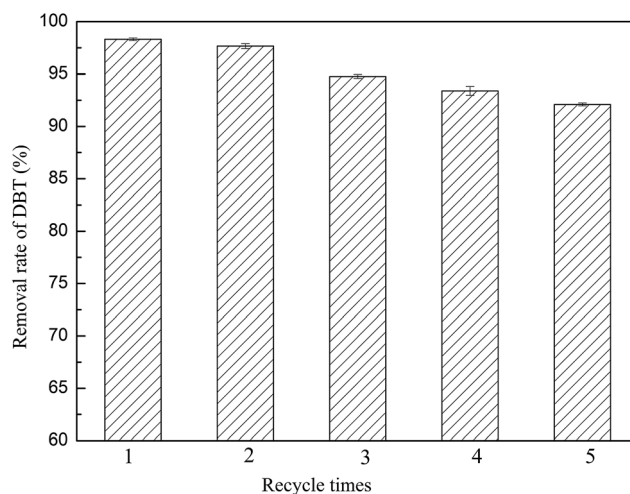


Fig. 12 The effects of reusing times on DBT removal of Mo/MMS catalyst.

data. The removal rate of sulfur of 98.1% (average of three replicates) was obtained by using optimized conditions which was nearly 0.9% lower than predicted value. The results were economically and technically feasible. Mokhtar *et al.*<sup>22</sup> reported the optimization of oxidative desulfurization of diesel fuel using RSM. About 84.5% sulfur removal could be achieved for 4,6-DMDBT under the optimum conditions: 3.0 of TBHP/S molar ratio, 48 °C and 31 min. 4,6-DMDBT removal in real diesel was lower (77%). It might be real oil containing a variety of sulfur compounds that make the oxidation difficult to occur. Therefore, RSM could be successfully applied in the optimization of oxidative desulfurization experiment to maximize the sulfur removal after comprehensive consideration of the affecting factors.

### 3.5. Reusing of catalyst

Since catalyst reusability is a key for industrial application, the reusability of Mo/MMS catalyst after each run of the reaction was researched under the optimum operating conditions (catalyst dosage of 0.50 g, temperature of 103 °C,  $O/S$  of 4.0, time of 62 min and the volume of model oil of 20 ml). The results were listed in Fig. 12, which indicated that the catalytic oxidative ability of the reused catalyst decreased from 98.1% to 92.2% after the catalyst was regenerated five times. The molybdenum content of the catalysts was 4.22%, 3.80%, 2.24%, and 1.10% during the second, third, fourth, and fifth uses of Mo/MMS catalyst, respectively. The results indicated that the cause of catalyst deactivation may be the leaching of molybdenum species. A. Chica *et al.*<sup>14</sup> analyzed the sulfur and metal contents of the  $MoO_x/Al_2O_3$  catalyst, the results showed that Mo had already leached out and the catalyst adsorbed large amounts of sulfones. Tian *et al.*<sup>34</sup> reported that the adsorption of the product ( $DBTO_2$ ) could be considered the main factor that caused a decrease in the catalytic activity of  $Mo/\gamma-Al_2O_3$  catalyst. Therefore, the adsorption of the oxidation products may be another reason for catalyst deactivation. As shown in Fig. 4, DBT

removal was 82.8% only by the extraction. It is possible that an extraction before the oxidation could improve removal rates and reduce the amount of catalyst necessary considerably.

## 4. Conclusions

Mo/MMS catalyst was successfully prepared by sorption method and characterized by SEM, XRD, FT-IR spectra and N<sub>2</sub> adsorption-desorption. Molybdenum was successfully immobilized on MMS and metal species were well dispersed on the surface of MMS.

Mo/MMS catalyst exhibited excellent desulfurization performance for DBT removal. DBT removal reached 97.5% in 60 min at a catalyst dosage of 0.50 g, temperature of 100 °C, O/S of 5.0 and the volume of model oil of 20 ml.

The Box-Behnken design was used to evaluate the influences of the main operating parameters, including oxidation temperature (40–120 °C), oxidation time (40–80 min) and O/S (1.0–5.0) on DBT removal in the process of ODS. The degree of importance was: O/S > oxidation temperature > oxidation time. The maximum DBT removal was 99.0% and 98.1% for the predicted and experimental data, respectively under the optimum conditions of oxidation temperature of 103 °C, oxidation time of 62 min and O/S of 4.0.

DBT removal dropped from 98.1% to 92.2% when the catalyst regenerated five rounds under the optimal removal conditions.

Mo/MMS catalyst showed the potential to be cost-effective and reusable in ODS.

## Acknowledgements

Financial support from the Nation Science Foundation of China (Grant Number: 51278464 and 51478172) and the Department of Science and Technology of Hunan Province (Project Contract No. 2014GK1012) is greatly appreciated.

## References

- D. Xie, Q. H. He, Y. Y. Su, T. W. Wang, R. F. Xu and B. X. Hu, *Chin. J. Catal.*, 2015, **36**(8), 1205–1213.
- W. N. W. Abdullah, R. Ali and W. A. W. A. Bakar, *J. Taiwan Inst. Chem. Eng.*, 2016, **58**, 344–350.
- J. M. Ramos, J. A. Wang, L. F. Chen, U. Arellano, S. P. Ramírez, R. Sotelo and P. Schachat, *Catal. Commun.*, 2015, **72**, 57–62.
- D. Zheng, W. S. Zhu, S. H. Xun, M. M. Zhou, M. Zhang, W. Jiang, Y. J. Qin and H. M. Li, *Fuel*, 2015, **159**, 446–453.
- A. Bazyari, A. A. Khodadadi, A. H. Mamaghani, J. Beheshtian, L. T. Thompson and Y. Mortazavi, *Appl. Catal., B*, 2015, **180**, 65–77.
- V. V. D. N. Prasad, K. E. Jeong, H. J. Chae, C. U. Kim and S. Y. Jeong, *Catal. Commun.*, 2008, **9**(10), 1966–1969.
- B. Jiang, H. W. Yang, L. W. Zhang, R. Y. Zhang, Y. L. Sun and Y. Huang, *Chem. Eng. J.*, 2016, **283**, 89–96.
- C. Y. Jiang, J. J. Wang, S. T. Wang, H. Y. Guan, X. H. Wang and M. X. Huo, *Appl. Catal., B*, 2011, **106**, 343–349.
- Z. E. A. Abdalla, B. S. Li and A. Tufail, *J. Ind. Eng. Chem.*, 2009, **15**(6), 780–783.
- X. H. Han, A. J. Wang, X. S. Wang, X. Li, Y. Wang and Y. K. Hu, *Catal. Commun.*, 2013, **42**(23), 6–9.
- Z. Y. Long, C. P. Yang, G. M. Zeng, L. Y. Peng, C. H. Dai and H. J. He, *Fuel*, 2014, **130**, 19–24.
- J. L. G. Gutiérrez, G. A. Fuentes, M. E. H. Terán, F. Murrieta, J. Navarrete and F. J. Cruza, *Appl. Catal., A*, 2006, **305**(1), 15–20.
- J. M. Fraile, C. Gil, J. A. Mayoral, B. Muel, L. Roldán, E. Vispe, S. Calderón and F. Puente, *Appl. Catal., B*, 2016, **180**, 680–686.
- A. Chica, A. Corma and M. E. Dómine, *J. Catal.*, 2006, **242**, 299–308.
- D. Valencia and T. Klimova, *Appl. Catal., B*, 2013, **129**(2), 137–145.
- X. M. Yan, B. F. Wang and J. J. Zhang, *Bioresour. Technol.*, 2015, **197**, 120–127.
- H. B. Li, L. Jing, Z. J. Yang, Q. Xu, C. T. Hou, J. Y. Peng and X. Y. Hu, *J. Hazard. Mater.*, 2011, **191**, 26–31.
- C. Jeon, *J. Ind. Eng. Chem.*, 2011, **17**(2), 321–324.
- W. J. Ding, W. S. Zhu, J. Xiong, L. Yang, A. M. Wei, M. Zhang and H. M. Li, *Chem. Eng. J.*, 2015, **266**, 213–221.
- W. N. A. W. Mokhtar, W. A. W. A. Bakar, R. Ali and A. A. A. Kadir, *J. Ind. Eng. Chem.*, 2015, **30**, 274–280.
- M. Luo, Y. X. Guan and S. J. Yao, *Chin. J. Chem. Eng.*, 2013, **21**(2), 185–191.
- W. N. A. W. Mokhtar, W. A. W. A. Bakar, R. Ali and A. A. A. Kadir, *Fuel*, 2015, **161**, 26–33.
- N. Jose, S. Sengupta and J. K. Basu, *Fuel*, 2011, **90**(2), 626–632.
- T. A. Zepeda, B. Pawelec, J. N. Díaz de León, J. A. de los Reyes and A. Olivas, *Appl. Catal., B*, 2012, **111**(3), 10–19.
- Y. M. Ni, A. M. Sun, X. L. Wu, J. L. Hu, T. Li and G. X. Li, *Chin. J. Chem. Eng.*, 2011, **19**(3), 439–445.
- F. Wang, Z. Q. Zhang, J. Yang, L. P. Wang, Y. Lin and Y. Wei, *Fuel*, 2013, **107**(9), 394–399.
- V. Huleaa, A. L. Maciucă, F. Fajula and E. Dumitriu, *Appl. Catal., A*, 2006, **313**(2), 200–207.
- X. Zhou, C. Zhao, J. Yang and S. Zhang, *Energy Fuels*, 2006, **21**(1), 7–10.
- J. H. Qiu, G. H. Wang, Y. Q. Zhang, D. L. Zeng and Y. Chen, *Fuel*, 2015, **147**, 195–202.
- N. Zang, X. M. Qian, P. Huang and C. M. Shu, *Thermochim. Acta*, 2013, **568**(35), 175–184.
- M. Zhang, W. S. Zhu, S. H. Xun, H. M. Li, Q. Q. Gu, Z. Zhao and Q. Wang, *Chem. Eng. J.*, 2013, **220**(6), 328–336.
- L. Tang, G. Q. Luo, M. Y. Zhu, L. H. Kang and B. Dai, *J. Ind. Eng. Chem.*, 2013, **19**(2), 620–626.
- X. X. Han and L. X. Zhou, *Chem. Eng. J.*, 2011, **172**(1), 459–466.
- Y. J. Tian, Y. Yao, Y. H. Zhi, L. J. Yan and S. X. Lu, *Energy Fuels*, 2015, **29**, 618–625.